JOURNAL OF GUIDANCE, CONTROL, AND DYNAMICS
Vol. 25, No. 1, January–February 2002

Analysis of Rotorcraft Flight Dynamics in Autorotation

S. S. Houston*
University of Glasgow, Glasgow, Scotland G12 8QQ, United Kingdom

Autorotation is a flight state whereby no powerplant torque is applied to the main rotor of a rotorcraft. For helicopters, autorotation is an abnormal mode of operation utilized in descending flight following total power failure. However it is the normal mode of operation for autogyros. It is common in helicopter mathematical modeling to assume constant rotorspeed, but this is invalid in autorotation. Introduction of the rotorspeed degree of freedom in modeling gives rise to an additional mode and coupling with the existing rigid-body modes. This paper therefore aims to explore the development of generic analytical expressions, exposing the role of the rotorspeed degree of freedom in modifying the classical rigid-body modes of motion. The analytical expressions are verified by quantifying their validity using autogyro derivatives obtained from a full nonlinear individual blade model. Comparison with the helicopter case then extends the generality and applicability of the analysis. It is concluded that there is an intimate relationship between the rotorspeed and low frequency rigid-body modes of rotorcraft in autorotation. The analytical expressions highlight the essence of coupled rotorspeed and rigid-body dynamics in autorotation, clearly identifying the conditions under which this relationship is stabilizing or otherwise.

Nomenclature

A	=	linearized model system matrix; stability cubic coefficient
A_{11}, etc.	=	minors of linearized system matrix
a_{ph}, b_{ph}	=	phugoid mode stability quadratic coefficients
a_{11}, a_{12}, etc	=	elements of low-order model system matrix
B	=	linearized model control matrix; stability cubic coefficient
B_1, B_2	=	minors of linearized control matrix
C	=	stability cubic coefficient
D, L	=	blade element drag and lift, N
M_u, M_w, etc.	=	pitching moment derivatives, 1/(ms), etc.
Q_u, Q_w, etc.	=	rotor torque derivatives, 1/(ms^2), etc.
q	=	pitch rate, rad/s
U_p, U_t	=	normal and tangential blade element velocities, m/s
u, w	=	translational velocity components along body axes, m/s
$\underline{u}$	=	control vector
X_u, X_w, etc.	=	longitudinal body axis acceleration derivatives, 1/s, etc.
$\underline{x}$	=	state vector
x_{blade}	=	blade element Ox axis
x_1, x_2	=	subspace of linearised model state vector
Z_u, Z_w, etc.	=	vertical body axis acceleration derivatives, 1/s, etc.
δA, δB, δC	=	changes to stability cubic coefficients as a result of coupling with rotorspeed degree of freedom
δa_{ph}, δb_{ph}	=	changes to phugoid mode stability quadratic coefficients as a result of coupling with rotorspeed degree of freedom
δU_p	=	perturbation in blade element normal velocity, m/s
η_s	=	longitudinal stick position, % (0% fully forward)
θ	=	pitch attitude, rad
θ_0	=	main rotor collective pitch, rad
λ	=	stability root
λ_Ω	=	rotorspeed mode stability root
ϕ, $\delta\phi$	=	blade element inflow angle; perturbation in blade element inflow angle, rad
ω_{sp}	=	short period mode approximation undamped natural frequency

Received 26 September 2000; revision received 10 April 2001; accepted for publication 16 April 2001.

*Senior Lecturer, Department of Aerospace Engineering. Member AIAA.

Introduction

AUTOROTATION is an aerodynamic condition whereby the angular velocity of a rotor is sustained by airflow, rather than by means of engine torque applied to the shaft. Helicopters use autorotation following total power failure, but for autogyros it is the normal mode of operation. Glauert's seminal work on autorotation[1] shows clearly that rotorspeed is a function of load factor and the axial component of rotor translational velocity. Pilots of rotary-wing aircraft are familiar with such behavior, although analysis of the impact of autorotation on flight dynamics is absent from the literature. Recently, interest in autogyro behaviour has produced data from mathematical modeling and flight experiments.[2–5] These data represent a sound framework for the analysis of the impact of the rotorspeed degree of freedom on the rigid-body modes and therefore handling qualities of rotorcraft in autorotation.

The objective of this paper is to explore the coupling between the rotorspeed degree of freedom and aircraft longitudinal rigid-body modes of motion, thereby contributing to a sparse literature on the subject, particularly for helicopters. The aims are as follows: first, to use the method of weakly coupled systems[6] to synthesise approximations to the rigid-body modes in terms of stability derivatives arising from inclusion of rotorspeed in the conventional model structure; second, to use these expressions to expose the role of the rotorspeed degree of freedom in modifying the classical rigid-body modes; third, to verify the analysis using data from a simulation mathematical model configured as an autogyro; and finally, to apply the analysis to a conventional helicopter.

Background

Recent work on the flight mechanics of autogyros has highlighted the importance of the rotorspeed degree of freedom in the simulation and analysis of rotorcraft in autorotation.[2–5] This work has shown that the longitudinal modes of motion are essentially similar to classical fixed-wing short-period and phugoid behavior, in terms of frequency and content. However, the model structure requires to be augmented by inclusion of the rotorspeed degree of freedom, resulting in an additional mode. Models identified from flight experiments using system identification methods[3] as well as those reduced from a fully nonlinear individual blade/blade element mathematical model[5] indicate a degree of coupling between the classical behaviour and this additional rotorspeed mode. The augmented model

structure introduces a new primary damping term and two groups of coupling derivatives: body/rotorspeed and rotorspeed/body.

The method of weakly coupled systems[6] provides a suitably rigorous analytical tool for unravelling the coupled behavior of multi-degree-of-freedom systems. In Milne's approach the natural separation of the various modes in terms of frequency is used as the basis of a series of low-order approximations to the actual modal behavior. These approximations, by virtue of their low order, can expose with clarity the factors influencing modal characteristics. The method has been applied successfully to the analysis of helicopter rigid-body modes.[7] The recent autogyro work[3,5] indicates that frequency separation between the modes exists, allowing direct application of Milne's method to this problem.

Analysis

The model structure is of conventional state-space form, that is,

$$\dot{\underline{x}} = A\underline{x} + B\underline{u} \tag{1}$$

where

$$A = \begin{bmatrix} X_u & X_w & X_q & X_\theta & X_\Omega \\ Z_u & Z_w & Z_q & Z_\theta & Z_\Omega \\ M_u & M_w & M_q & M_\theta & M_\Omega \\ 0 & 0 & 1 & 0 & 0 \\ Q_u & Q_w & Q_q & Q_\theta & Q_\Omega \end{bmatrix}, \qquad B = \begin{bmatrix} X_{\eta_s} \\ Z_{\eta_s} \\ M_{\eta_s} \\ 0 \\ Q_{\eta_s} \end{bmatrix} \tag{2}$$

$$\underline{x} = [u \quad w \quad q \quad \theta \quad \Omega]^T, \qquad \underline{u} = [\eta_s] \tag{3}$$

This constitutes the longitudinal subset of the conventional six-degree-of-freedomrigid-body flight mechanics model, with the important (and unique) addition of the rotorspeed degree of freedom. Reordering and partitioning Eq. (1) thus

$$\begin{bmatrix} \dot{x}_1 \\ \dot{x}_2 \end{bmatrix} = \begin{bmatrix} A_{11} & A_{12} \\ A_{21} & A_{22} \end{bmatrix} \begin{bmatrix} x_1 \\ x_2 \end{bmatrix} + \begin{bmatrix} B_1 \\ B_2 \end{bmatrix} u \tag{4}$$

where $x_1 = [w \quad q]^T$ and $x_2 = [u \quad \theta \quad \Omega]^T$ prepares the model for simple application of Milne's method, as follows:

$$\dot{x}_1 = A_{11}x_1 + A_{12}x_2 + B_1 u \tag{5}$$

$$\dot{x}_2 = A_{21}x_1 + A_{22}x_2 + B_2 u \tag{6}$$

where

$$A_{11} = \begin{bmatrix} Z_w & Z_q \\ M_w & M_q \end{bmatrix} \tag{7}$$

$$A_{12} = \begin{bmatrix} Z_u & Z_\theta & Z_\Omega \\ M_u & 0 & M_\Omega \end{bmatrix} \tag{8}$$

$$A_{21} = \begin{bmatrix} X_w & X_q \\ 0 & 1 \\ Q_w & Q_q \end{bmatrix} \tag{9}$$

$$A_{22} = \begin{bmatrix} X_u & X_\theta & X_\Omega \\ 0 & 0 & 0 \\ Q_u & 0 & Q_\Omega \end{bmatrix} \tag{10}$$

The partitioned system described by Eqs. (5–10) can be described as "weakly coupled" if the eigenvalue sets implied by the partitioning are widely separated in modulus, and the coupling matrices are in some sense small. Full description of the theory is to be found in Ref. 6, but for the purposes of this paper the consequences of weak coupling are that Eqs. (5) and (6) become

$$\dot{x}_1 = A_{11}x_1 + B_1 u \tag{11}$$

$$\dot{x}_2 = \left(A_{22} - A_{21}A_{11}^{-1}A_{12}\right)x_2 + \left(B_2 - A_{21}A_{11}^{-1}B_1\right)u \tag{12}$$

Equation (11) approximates the short-period behavior (the approximation does not include rotorspeed), whereas Eq. (12) approximates the phugoid and rotorspeed modes. References 3 and 5 indicate that there is no separation in modulus between rotorspeed and phugoid modes, and so no further partitioning of Eq. (12) into two simpler subsystems is possible. Additional simplification is made by neglecting the derivatives Q_q, Z_θ, and M_θ. Error bounds associated with identification of Q_q from flight test are so large as to suggest that it may be inappropriate to include in the model structure,[3] whereas the contributions of Z_θ and M_θ to the modes can be verified as normally very small. The elements of the system matrix of Eq. (12) are then

$$A_{22} - A_{21}A_{11}^{-1}A_{12} = \begin{bmatrix} a_{11} & a_{12} & a_{13} \\ a_{21} & a_{22} & a_{23} \\ a_{31} & a_{32} & a_{33} \end{bmatrix} \tag{13}$$

where

$$a_{11} = X_u - \frac{X_w(M_qZ_u - Z_qM_u) + X_q(M_uZ_w - Z_uM_w)}{\omega_{sp}^2}$$

$$a_{12} = X_\theta$$

$$a_{13} = X_\Omega - \frac{X_w(M_qZ_\Omega - Z_qM_\Omega) + X_q(M_\Omega Z_w - Z_\Omega M_w)}{\omega_{sp}^2}$$

$$a_{21} = -\frac{M_uZ_w - Z_uM_w}{\omega_{sp}^2}$$

$$a_{22} = 0$$

$$a_{23} = -\frac{M_\Omega Z_w - Z_\Omega M_w}{\omega_{sp}^2}$$

$$a_{31} = Q_u - \frac{Q_w(M_qZ_u - Z_qM_u)}{\omega_{sp}^2}$$

$$a_{32} = 0$$

$$a_{33} = Q_\Omega - \frac{Q_w(M_qZ_\Omega - Z_qM_\Omega)}{\omega_{sp}^2}$$

And the characteristic equation is

$$\lambda^3 - (a_{11} + a_{33})\lambda^2 + (a_{11}a_{33} - a_{21}a_{12} - a_{31}a_{13})\lambda + a_{12}(a_{21}a_{33} - a_{31}a_{23}) = 0 \tag{14}$$

Note that the rotorspeed derivatives pervade all three coefficients in this cubic equation, and because no further partitioning of the subsystem matrix is possible no simple, direct relationships can be synthesized to relate phugoid and rotorspeed mode characteristics to terms in Eq. (13).

However, the sensitivity of the modes to changes in the derivatives can be established by a perturbation analysis of Eq. (14). Noting that Eq. (14) can be written as

$$\lambda^3 + A\lambda^2 + B\lambda + C = 0 \tag{15}$$

$$(\lambda - \lambda_\Omega)\left(\lambda^2 + a_{ph}\lambda + b_{ph}\right) = 0 \tag{16}$$

then the following linearized relationships can be determined:

$$\delta a_{ph} = \delta A\left(1 + \frac{\lambda_\Omega^2}{\lambda_\Omega A - b_{ph}}\right) + \delta B\left(\frac{\lambda_\Omega}{\lambda_\Omega A - b_{ph}}\right) + \delta C\left(\frac{1}{\lambda_\Omega A - b_{ph}}\right) \tag{17}$$

$$\delta b_{ph} = \delta A\left(1 - \frac{A}{\lambda_\Omega A - b_{ph}}\right)\lambda_\Omega + \delta B\left(1 - \frac{A\lambda_\Omega}{\lambda_\Omega A - b_{ph}}\right) + \delta C\left(\frac{-A}{\lambda_\Omega A - b_{ph}}\right) \tag{18}$$

$$\delta\lambda_\Omega = \delta A\left(\frac{\lambda_\Omega^2}{\lambda_\Omega A - b_{\text{ph}}}\right) + \delta B\left(\frac{\lambda_\Omega}{\lambda_\Omega A - b_{\text{ph}}}\right) + \delta C\left(\frac{1}{\lambda_\Omega A - b_{\text{ph}}}\right) \tag{19}$$

where δ signifies changes caused by the presence of those terms in the cubic that couple the rotorspeed degree of freedom with the phugoid mode, that is, $\delta A = 0$, $\delta B = -a_{31}a_{13}$, and $\delta C = -a_{31}a_{23}a_{12}$. These equations can be used to describe the relationships between the derivatives specific to inclusion of the rotorspeed degree of freedom and the phugoid mode. Root locus plots for the full system then provide an important verification that the essential features of the system are encapsulated by these approximations.

Results

The nonlinear individual blade/blade element rotorcraft model described in Ref. 5 is generic, requiring only an appropriate collection of data to render the simulation type specific. The model has been validated against flight-test data in both helicopter[8,9] and autogyro configurations.[5] However, validation of helicopters in autorotation has not been possible because of lack of data in this flight condition, although model functionality has been verified by ensuring that performance curves, e.g., relating rate of descent and airspeed,[10] have the correct appearance. Autogyro validation has shown that the model emulates satisfactorily the variability in rotorspeed that is a consequence of operation in autorotation. As a result, the results focus on this aircraft as the model has a defined level of validity in this application.

Verification of Approximations

The VPM M16 autogyro was simulated for a mass of 425 kg in steady level flight at 60 kn and a density altitude of 2000 ft. The model was linearized numerically, and the resulting stability and control derivatives are given next, reordered, and partitioned in accordance with Eq. (4):

$$\begin{bmatrix}\dot{w}\\ \dot{q}\\ \dot{u}\\ \dot{\theta}\\ \dot{\Omega}\end{bmatrix} = A\begin{bmatrix}w\\ q\\ u\\ \theta\\ \Omega\end{bmatrix} + B\eta_s \tag{20}$$

where

$$A = \begin{bmatrix}-1.2019 & 28.6824 & -0.2336 & 0.1218 & -0.3143\\ -0.0239 & -1.001 & -0.0010 & 0 & -0.0016\\ -0.2388 & 0.6993 & -0.2579 & -9.2219 & -0.0518\\ 0 & 1 & 0 & 0 & 0\\ 0.6692 & -1.5088 & 0.1557 & 0 & -0.1052\end{bmatrix}$$

$$B = \begin{bmatrix}-29.7685\\ 12.4604\\ -15.0729\\ 0\\ -19.1078\end{bmatrix}$$

Table 1 shows the eigenvalues of this system, together with those of the approximate models described by Eqs. (11) and (12). It can be seen that the essential requirement of the weakly coupled systems approach is met, that is, that the modes must be widely separated in modulus. The approximations are good representations of mode damping and frequency and therefore form a suitable basis for analysis.

Table 1 Comparison of approximate and exact modes

Mode	Exact	Approximate
Short period	-1.0641 ± 0.8636i	-1.1015 ± 0.8218i
Phugoid	-0.0737 ± 0.1335i	-0.0901 ± 0.1264i
Rotorspeed	-0.2895	-0.2757

Table 2 Rotorspeed coupling terms and approximate system modes

System	Phugoid mode	Rotorspeed mode
Eq. (21)	-0.0901 ± 0.1264i	-0.2757
Eq. (21), no rotorspeed coupling	-0.1115 ± 0.0937i	-0.1052

Coupling with Rotorspeed

Using the approximation given by Eq. (13), the values in Eq. (20) give

$$A_{22} - A_{21}A_{11}^{-1}A_{12} = \begin{bmatrix}-0.2229 & -9.2219 & -0.0100\\ 0.0023 & 0 & 0.0030\\ 0.0624 & 0 & -0.2329\end{bmatrix} \tag{21}$$

Table 2 compares the eigenvalues of this system with those that would pertain if the rotorspeed and rotor torque derivatives were zero.

The approximation shows that coupling between the body and rotorspeed degrees of freedom serves to destabilize the phugoid mode by almost 20% and increase its undamped natural frequency by 35%. The rotorspeed mode damping however benefits from the coupling between these degrees of freedom, as its damping is increased by 160%.

Consideration of Table 2, together with Eqs. (13), (20), and (21), identifies clearly the sources of the increased damping of the rotorspeed mode. First, the primary damping derivative $Q_\Omega = -0.1052$ is augmented by the term

$$-\frac{Q_w(M_q Z_\Omega - Z_q M_\Omega)}{\omega_{\text{sp}}^2} \tag{22}$$

This is responsible for increasing its value to -0.2329. Second, the terms a_{13}, a_{23}, and a_{31} redistribute the remainder from the phugoid mode damping. Their role can be identified using Eqs. (14) and (17). A numerical audit of the terms in Eq. (21) confirms that δB is negligibly small. Hence, although the coupling derivative X_Ω is nonzero its influence is diminished by other compensating terms, principally the effect of X_w. The focus is then on cubic coefficient C, and writing

$$\delta C = -a_{12}a_{31}a_{23} \tag{23}$$

then the presence of these coupling terms gives $\delta C > 0$, that is, $\delta a_{\text{ph}} < 0$ and $\delta b_{\text{ph}} > 0$, which is verified in Table 2.

Role of Rotor Torque Derivatives Q_u and Q_w

Figure 1 shows a simplified representation of the forces acting on a blade element in equilibrium and perturbed flight. If the perturbation is assumed to be small, then blade lift and drag have approximately the equilibrium values, simply rotated by $\delta\phi$. The in-plane force is increased by $\delta X = L\delta\phi$, tending to increase the rotorspeed. Because the autogyro rotor is tilted aft relative to the airframe typically by 10 deg, then perturbations in u as well as w will give rise to δU_p. This means that the fundamental physics of autorotation are such that $Q_u > 0$, $Q_w > 0$, with $Q_u < Q_w$. Q_w serves to bring additional damping to the low-frequency subsystem comprising phugoid and rotorspeed modes, but it also redistributes this damping between these modes through the coupling term a_{31}. Because Q_u only appears in a_{31}, it acts purely to distribute subsystem damping between the modes, although in this case its effect is mitigated by Z_u because Q_w is always positive.

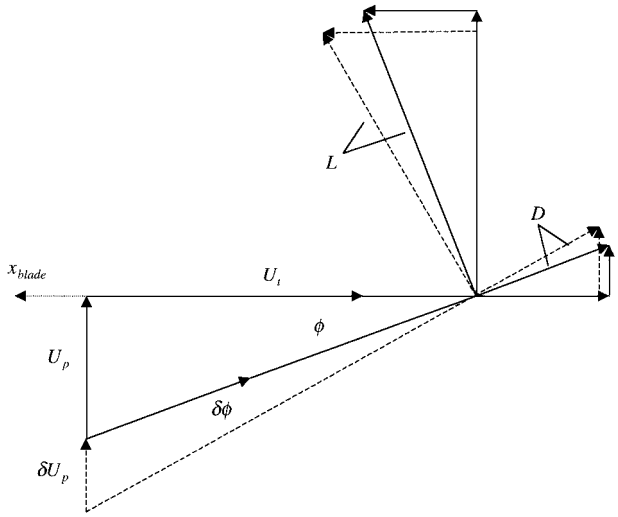

Fig. 1 Schematic of blade element forces in equilibrium and distrubed flight.

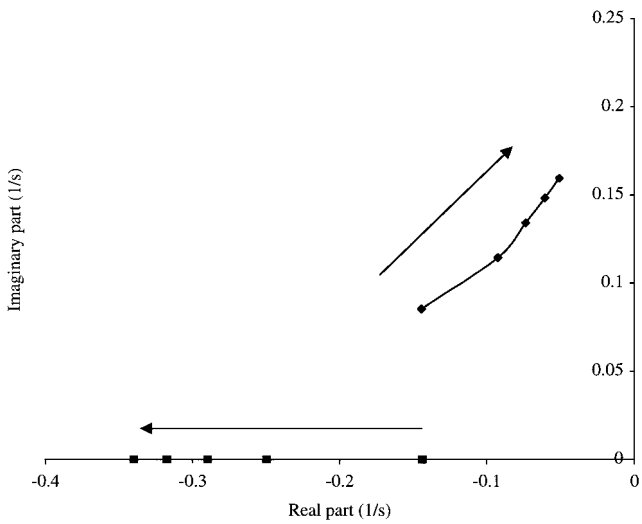

Fig. 2 Root locus of autogyro phugoid and rotorspeed modes: increasing Q_u; ♦, phugoid, and ■, rotorspeed.

Without Q_u, a_{31} would be negative, and Eq. (23) then shows that the phugoid mode damping would be substantially increased at the expense of rotorspeed mode damping. Figure 2 is the root locus plot for varying Q_u between 0.06 and 0.26. As phugoid mode damping is decreased with increasing Q_u, that of the rotorspeed mode is increased and vice versa.

Pitching-Moment Perturbations Caused by Rotorspeed Changes (M_Ω)

The derivative M_Ω has an important role to play for two reasons. First, unlike the other rotorspeed and torque derivatives that will be largely invariant for a given aircraft, M_Ω can vary with the position of the center-of-mass. Second, it can be seen from the preceding section that M_Ω has an intimate role to play both in redistributing damping from phugoid to rotorspeed modes, as well as augmenting the primary rotorspeed damping through coupling with other terms.

For example, if

$$M_\Omega = Z_\Omega M_w / Z_w \tag{24}$$

then $a_{23} = 0$, that is, $\delta C = 0$. There will be no parasitic redistribution of phugoid damping to the rotorspeed mode. For the model given by Eq. (20), this would require $M_\Omega = -0.00625$. A secondary effect of such a change to M_Ω is increased primary rotorspeed damping. However, if

$$M_\Omega = M_q Z_\Omega / Z_q \tag{25}$$

Table 3 Impact of rotorspeed coupling terms on approximate system modes

System	Phugoid mode	Rotorspeed mode
Eq. (21)	-0.0901 ± 0.1264i	-0.2757
Eq. (21), $M_\Omega = -0.00625$	-0.1144 ± 0.0925i	-0.2744
Eq. (21), $M_\Omega = 0.01097$	-0.0255 ± 0.1736i	-0.2771

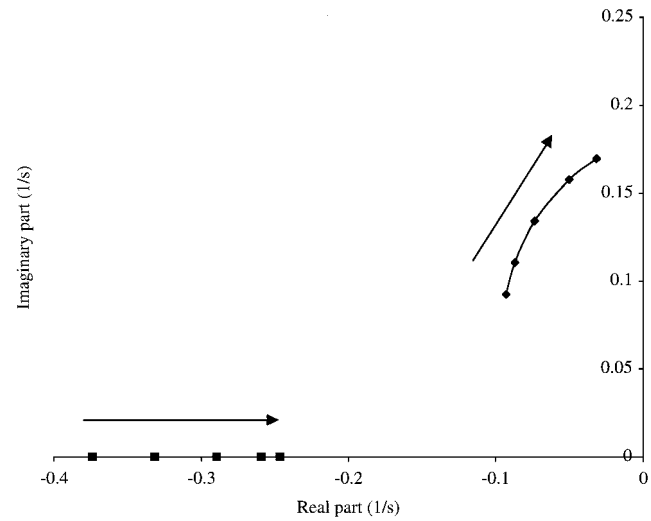

Fig. 3 Root locus of autogyro phugoid and rotorspeed modes: increasing M_Ω; ♦, phugoid, and ■, rotorspeed.

for which $M_\Omega = 0.01097$, then two adverse changes take place. First, the primary rotorspeed damping derivative is not augmented. This means that a_{33} is reduced, that is, $\delta A < 0$. Equations (17) and (19) indicate that the consequence of this is $\delta a_{\text{ph}} < 0$ and $\delta\lambda_\Omega > 0$, that is, both phugoid and rotorspeed modes are destabilized. However, the coupling term a_{23} is increased substantially, and as has already been seen this will redistribute damping from the phugoid to the rotorspeed mode. Although this further worsens the phugoid mode damping and increases the frequency, it does serve to augment the rotorspeed mode. These changes are verified and quantified in Table 3, and Fig. 3 is the root locus plot for increasing M_Ω from -0.0096 to $+0.0096$, which confirms the role of this derivative in the stability of both phugoid and rotorspeed modes.

Helicopter Case

Although the model has not been validated for helicopter operation in autorotation, it is argued that the autogyro validation results are of relevance and significance to the simulation of helicopters in autorotation because of the generic nature of the simulation code. However, unlike the autogyro, the helicopter sustains autorotation by means of descending flight, and therefore increasing air density may, over a period of time, adversely impact on the veracity of any linearization. It is therefore appropriate to quantify and understand limitations in the linearized model with respect to the full nonlinear simulation. Configuration data for the Puma helicopter were used to simulate a steady 1900 ft/min descent at 70 kn indicated airspeed, at density altitude of 4000 ft and a mass of 5500 kg. Figure 4 compares the response of the full nonlinear individual blade/blade element model with that of the linearized version. The input is a collective pitch doublet of 2-s period, and the amplitude is 10% of the available travel. In addition, the air density is fixed in the nonlinear model at the value pertinent to the trim point. It is clear that the linearized model accurately captures mode characteristics, with some nonlinearity being present in terms of the amplitude of the response. However, in Fig. 5 air density is free to vary with flight condition and increases as the aircraft descends from 4000 to almost 2000 ft. It is clear in this case that although the linearized model again captures nonlinear mode characteristics in terms of damping and frequency, the nonlinear rotorspeed and true airspeed responses

gradually decrease with time, albeit by very small amounts. The true airspeed decrease is consistent with an almost constant indicated airspeed. It is argued that in this case linearized modeling is appropriate for capturing modal characteristics of a helicopter in autorotation, and the small-perturbation analysis can proceed.

The stability and control derivatives are given next, reordered, and partitioned in accordance with Eq. (4):

$$\begin{bmatrix} \dot{w} \\ \dot{q} \\ \dot{u} \\ \dot{\theta} \\ \dot{\Omega} \end{bmatrix} = A \begin{bmatrix} w \\ q \\ u \\ \theta \\ \Omega \end{bmatrix} + B\theta_0 \tag{26}$$

where

$$A = \begin{bmatrix} -0.6562 & 36.2593 & -0.0183 & 0.0 & -0.3864 \\ -0.0084 & -0.7597 & 0.0049 & 0 & -0.0062 \\ -0.0151 & -9.6090 & -0.0129 & -9.2081 & 0.0379 \\ 0 & 1 & 0 & 0 & 0 \\ 0.1056 & -0.0604 & 0.0034 & 0 & -0.0677 \end{bmatrix}$$

$$B = \begin{bmatrix} -94.1647 \\ 5.7640 \\ -4.2271 \\ 0 \\ -0.2007 \end{bmatrix}$$

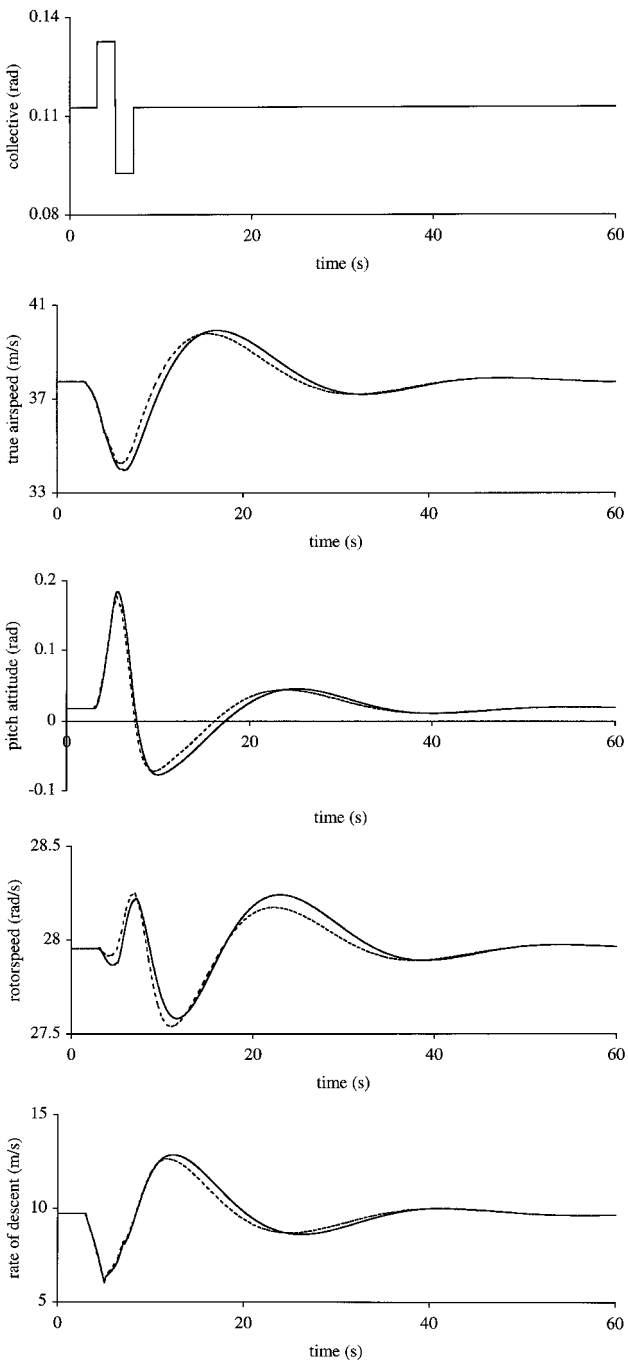

Fig. 4 Linear and nonlinear model response to collective input (fixed air density): ——, nonlinear, and – – –, linear.

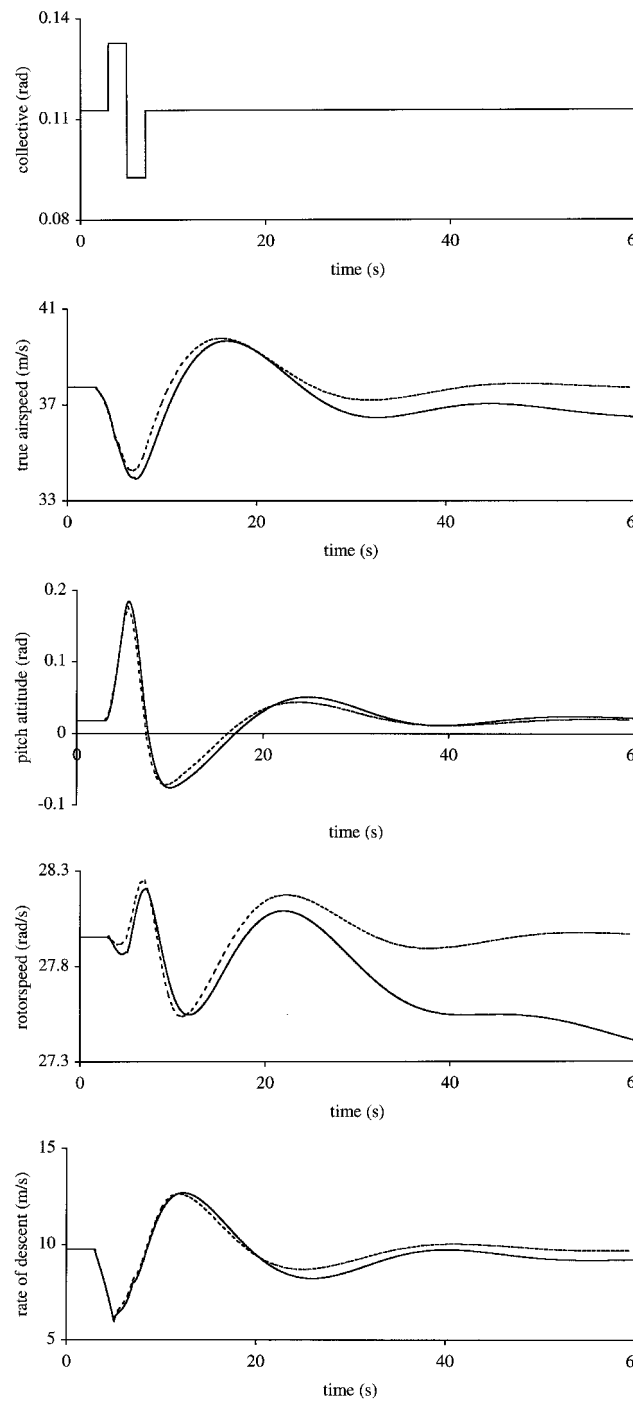

Fig. 5 Linear and nonlinear model response to collective input (varying air density): ——, nonlinear, and – – –, linear.

Table 4 Comparison of approximate and exact modes

Mode	Exact	Approximate
Short period	-0.6483 ± 0.5317i	-0.7080 ± 0.5361i
Phugoid	-0.0237 ± 0.1931i	-0.0288 ± 0.1913i
Rotorspeed	-0.1525	-0.1346

Table 5 Rotorspeed coupling terms and approximate system modes

System	Phugoid mode	Rotorspeed mode
Eq. (27)	-0.0288 ± 0.1913i	-0.1346
Eq. (27), no rotorspeed coupling	-0.0283 ± 0.1947i	-0.0677

Table 4 shows the eigenvalues of this system, together with those of the approximate models described by Eqs. (11) and (12). As with the autogyro configuration, the modes are widely separated in modulus, and the approximations form a suitable basis for analysis.

Using the approximation given by Eq. (13), the values in Eq. (26) give

$$A_{22} - A_{21}A_{11}^{-1}A_{12} = \begin{bmatrix} -0.0565 & -9.2081 & 0.0053 \\ 0.0042 & 0 & -0.0010 \\ 0.0250 & 0 & -0.1357 \end{bmatrix} \quad (27)$$

Table 5 compares the eigenvalues of this system with those that would pertain if the rotorspeed and rotor torque derivatives were zero.

The effect of including rotorspeed and torque derivatives on the rotorspeed mode is similar to that for the autogyro in that damping is increased. However, the effect on the phugoid mode is negligible. The source of the rotorspeed mode is the primary damping derivative $Q_\Omega = -0.0677$ augmented by the term

$$-Q_w(M_q Z_\Omega - Z_q M_\Omega)/\omega_{\text{sp}}^2 = -0.0681 \quad (28)$$

This raises its value to -0.1357, consistent with Eq. (27). Unlike the autogyro case however, the terms a_{13}, a_{23}, and a_{31} are such that $\delta C \approx 0$. Equations (14) and (17) then show that $\delta a_{\text{ph}} \approx 0$ and $\delta b_{\text{ph}} \approx 0$, verified by Table 5. This is despite the fact that on inspection the rotorspeed and rotor torque coupling derivatives in Eq. (26) are not negligible. The analysis has identified how a particular combination of derivatives can have an insignificant effect on the phugoid mode, despite the fact that the individual derivatives themselves may be nontrivial.

Unlike the autogyro case, $Q_u \approx 0$. This is because the helicopter rotor is effectively aligned with the airframe so that changes in u (unlike w) will not give rise to a change in the axial velocity and hence torque. However, the coupling term a_{31} remains positive, but for a quite dissimilar reason to that of the gyroplane $-M_u$ is large and positive. The potential contribution of M_u to redistribution of rotorspeed and phugoid mode damping is ameliorated however by small a_{23}, but this may not generally be the case for other helicopters. Figure 6 is the root locus plot for variations in Q_u of ± 0.1, that is, up to almost the same magnitude as Q_w, which is physically unrealistic. The results confirm the analysis that the damping of these modes is much less sensitive than the autogyro to changes in Q_u. However, Fig. 7 shows that M_Ω has the same impact on this helicopter as it has for the autogyro. The arrows indicate the trend from $M_\Omega = -0.0186$ to $M_\Omega = 0.0062$.

The final consideration in the analysis of the helicopter is the derivative X_q. Although it is not a consequence of introducing the rotorspeed degree of freedom, it is quite dissimilar from the level flight value as a consequence of the high rate of descent in autorotation. The approximation given by Eq. (13) shows that X_q appears in a_{11} and a_{13}. With regard to a_{11}, X_q, can either augment or diminish X_u, that is, augment or diminish phugoid mode damping. From the values given in Eq. (26), it can be shown that $X_q = -9.6090$ is largely responsible for increasing the drag damping term in Eq. (27) from -0.0129 to -0.0565. M_u again has a role to play because

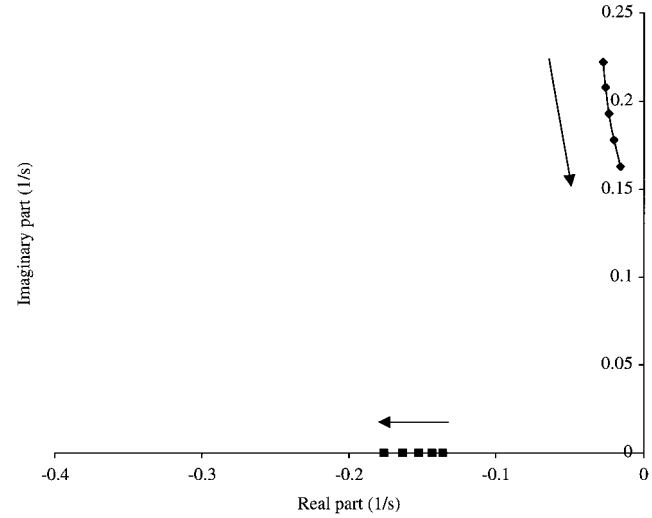

Fig. 6 Root locus of helicopter phugoid and rotorspeed modes: increasing Q_u; ♦, phugoid, and ■, rotorspeed.

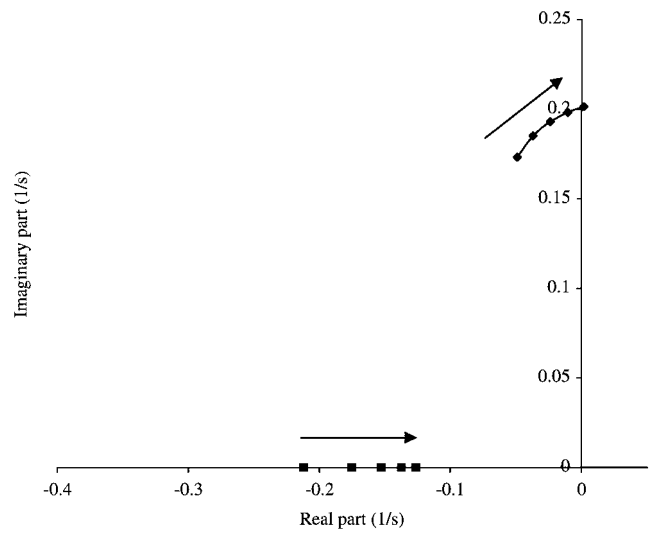

Fig. 7 Root locus of helicopter phugoid and rotorspeed modes: increasing M_Ω; ♦, phugoid, and ■, rotorspeed.

the approximation (13) shows that the presence of a substantially negative X_q will only tend to diminish phugoid mode damping if $M_u Z_w - Z_u M_w > 0$, which can occur if M_u is negative.

Discussion

Insight provided by the weakly coupled systems method lays bare the various complex interrelationships between the derivatives that give rise to the modal characteristics. The analysis can establish the conditions under which inclusion of the rotorspeed degree of freedom will stabilize, or destabilize, the low-frequency body mode. It is accepted that the approximations require a degree of familiarity on the part of the reader, but they preserve the generality lost with a numerical sensitivity analysis. A number of derivatives, either singly or in combination, clearly have an important role to play, specifically Q_u, Q_w, X_q, and M_Ω. Whether or not these derivatives serve to stabilize or destabilize modes often depends on other aircraft characteristics not a consequence of autorotation, such as M_q or M_u, and so on. For example, Q_w will only augment damping of the low-frequency modes if $M_q Z_\Omega > Z_q M_\Omega$, but it is difficult to envisage a rotorcraft configuration for which this will not be the case. Unlike the helicopter, the autogyro rotor is tilted aft relative to the airframe, leading to some derivatives being significantly larger in magnitude such as Q_u, Z_u, X_Ω, and X_w. However for the helicopter the high rate of descent in autorotation results in a large negative X_q. Despite these significant differences, the essential results of the autogyro and

helicopter case studies are similar—the rotorspeed mode damping is enhanced by coupling with the body degrees of freedom, while the low-frequency body mode (phugoid) may show little change.

The derivative M_Ω also has an important role to play because it can be varied with loading condition, and the results presented here confirm the intuitive static stability consideration that $M_\Omega < 0$ will tend to be stabilizing. This implies that the main rotor thrust line passes behind the center-of-mass, which is not unreasonable for a well-designed autogyro or a hingeless rotor helicopter with a high equivalent hinge offset. However, it is likely to be the case that some rotorcraft will have a center-of-mass close to the main rotor thrust line and hence negligible M_Ω. The analytical expressions and root locus results then show that the phugoid mode will tend to be destabilized by coupling with the rotorspeed degree of freedom. The salient role of M_Ω coupling the phugoid and rotorspeed modes in autorotation may be of significance if pilot control strategy involves loop closure using rotorspeed. For autogyros or helicopters feedback of rotorspeed to the longitudinal control is likely to render increasingly negative M_Ω. Such a control strategy may be unlikely for helicopters, although this is not the case for autogyros. However, with helicopters pilot use of main rotor collective to control rotorspeed is more likely, and for high equivalent hinge offset main rotors that exhibit strong pitching moment changes with collective pitch movement M_Ω will be rendered destabilizing.

Finally, the approach outlined in this paper constitutes a rigorous, clearly defined, and consistent framework for the generalized analysis of the role of additional terms that arise as a result of operation in autorotation. The strength of such an analytical approach is that it preserves the generality lost with say a numerical sensitivity analysis, although increasing system complexity can render the latter an expedient method. For example, the helicopter and autogyro cases examined both had positive angle of attack stability ($M_w < 0$). This is not generally the case with rotorcraft, and as M_w becomes more positive the short-period oscillation degenerates into two aperiodic modes, one of large modulus, the other small. In the presence of the rotorspeed degree of freedom, increasingly positive M_w results in the latter eigenvalue merging rapidly with the rotorspeed mode to form a second low-modulus oscillation, indistinguishable from the existing phugoid mode in eigenstructure. Figure 8 illustrates this effect for the helicopter case, with M_w increasing from -0.0084 to $+0.0062$. The approximations developed here are no longer valid and have to be reformulated to reflect the different modal structure, specifically the quartic, as opposed to cubic characteristic of the low modulus modes of motion. However, the cubic approximation is likely to be valid for a large class of contemporary helicopter configurations that will tend to exhibit $M_w < 0$ as a result of careful empennage design and relatively soft flapwise or low flap hinge offset rotors.

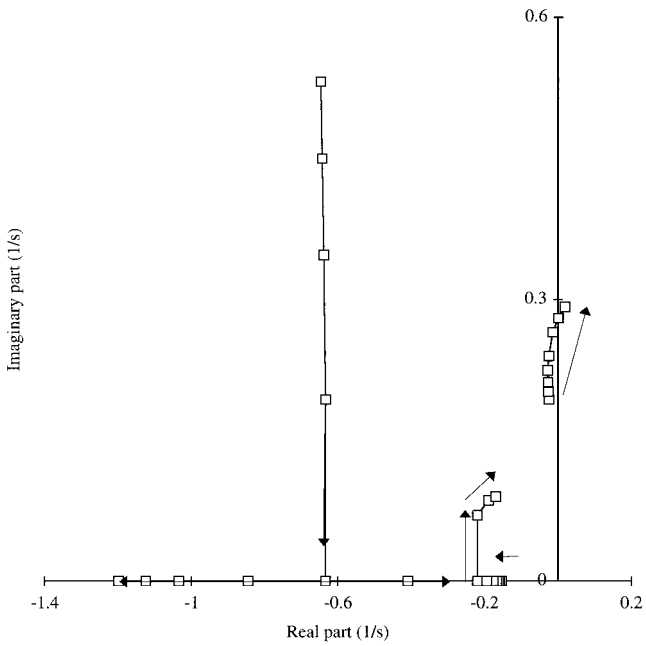

Fig. 8 Root locus of helicopter short-period, phugoid, and rotorspeed modes: increasing M_w.

Conclusions

The method of weakly coupled systems can be used to derive analytical expressions that describe the complex nature of the interaction between rotorspeed and low-frequency rigid-body modes of rotorcraft in autorotation. These modes display an intimate relationship in which the pitching-moment change with rotorspeed has a major role to play in determining stability characteristics. Torque changes with flight condition can also increase or decrease damping and frequency of the low-frequency phugoid rigid-body mode for helicopters and autogyros. Use of the approximations with typical autogyro and helicopter simulation models, complimented by simple root loci, verifies the generality of the approach and confirms the integrity of the results.

References

[1] Glauert, H., "A General Theory of the Autogyro," Aeronautical Research Committee, Reports and Memoranda No. 1111, London, Nov. 1926.

[2] Houston, S. S., "Longitudinal Stability of Gyroplanes," *The Aeronautical Journal*, Vol. 100, No. 991, 1996, pp. 1–6.

[3] Houston, S. S., "Identification of Autogyro Longitudinal Stability and Control Characteristics," *Journal of Guidance, Control, and Dynamics*, Vol. 21, No. 3, 1998, pp. 391–399.

[4] Houston, S. S., "Identification of Gyroplane Lateral/Directional Stability and Control Characteristics from Flight Test," *Proceedings of the Institution of Mechanical Engineers*, Pt. G, Vol. 212, 1998, pp. 1–15.

[5] Houston, S. S., "Validation of a Rotorcraft Mathematical Model for Autogyro Simulation," *Journal of Aircraft*, Vol. 37, No. 3, 2000, pp. 203–209.

[6] Milne, R. D., "The Analysis of Weakly Coupled Dynamical Systems," *International Journal of Control*, Vol. 2, No. 2, 1965, pp. 171–199.

[7] Padfield, G. D., "On the Use of Approximate Models in Helicopter Flight Mechanics," *Vertica*, Vol. 5, No. 3, 1981, pp. 243–259.

[8] Houston, S. S., "Validation of a Non-Linear Individual Blade Rotorcraft Flight Dynamics Model Using a Perturbation Method," *The Aeronautical Journal*, Vol. 98, No. 977, 1994, pp. 260–266.

[9] Houston, S. S., "Validation of a Blade-Element Helicopter for Large-Amplitude Maneuvres," *Aeronautical Journal*, Vol. 101, No. 1001, 1997, pp. 1–7.

[10] Coyle, S., *The Art and Science of Flying Helicopters*, Arnold, London, 1996, pp. 164, 165.